Valleytronics, Carrier Filtering and Thermoelectricity in Bismuth: Magnetic Field Polarization Effects

Adrian Popescu[1,2] and Lilia M. Woods[3]

[1]*Center for Nanoscale Science and Technology, National Institute of Standards and Technology, Gaithersburg, MD 20899*

[2]*Maryland NanoCenter, University of Maryland, College Park, MD, 20742*

[3]*Department of Physics, University of South Florida, Tampa, FL 33620, USA*

Valley polarization of multi-valleyed materials is of significant interest for potential applications in electronic devices. The main challenge is removing the valley degeneracy in some controllable way. The unique properties of bismuth, including its anisotropic electronic structure and Dirac valley degeneracy, make this material an excellent system for valleytronics. We demonstrate theoretically that the direction of an externally applied magnetic field in the binary-bisectrix plane has a profound effect not only on the charge, but also on the thermal transport along the trigonal direction. The rotating field probes the electronic mass anisotropy and tunes the contribution from a particular Dirac valley in the electrical resistivity, Seebeck coefficient, and thermal conductivity at moderate temperatures and field strengths. We further show that the field polarization of the transport properties is accompanied by selective filtering of the carriers type providing further opportunities for thermoelectric transport control.

I. Introduction

Creating an imbalance in the energy bandstructure valleys is an interesting concept motivated by the potential of constructing multichannel devices with valley polarization properties[1-3]. Usually

two-dimensional materials, such as graphene, AlAs or Si surfaces, are envisioned for such manipulations[2-5]. However, recent experiments demonstrate that valley polarization effects are manifested in the measured angular oscillations of the electrical resistivity of bismuth as a function of the external magnetic field orientation.[6] This behavior suggests that tuning of each electronic valley contribution to the total resistivity is achievable in a wide temperature regime.

Here we present a model showing that the *charge and heat* currents can be valley-polarized with a magnetic field applied in the bismuth binary-bisectrix (bb) plane. We demonstrate that valleytronics is feasible for other transport characteristics along the trigonal direction, such as the Seebeck coefficient and thermal conductivity. Consequently, thermoelectricity exhibits preferential excitations, with the bismuth figure of merit being profoundly affected by the magnetic field orientation. The model is validated by interpreting existing experimental results for the bismuth resistivity along the trigonal direction [6].

II. Theoretical Approach

Bismuth is characterized by a rhombohedral crystal structure and a Fermi surface consisting of a hole carrier ellipsoid located around the trigonal axis (T-point) and three electron carrier ones almost perpendicular to the trigonal axis (L-points) (Figure 1). The electronic energy dispersion $\varepsilon_e(\mathbf{k})$ is described via a two-band, non-parabolic model[7]: $\varepsilon_e(\mathbf{k})(1+\frac{\varepsilon_e(\mathbf{k})}{\varepsilon_g})=\frac{\hbar^2}{2m_0}\mathbf{k}\underline{m}_e^{-1}\mathbf{k}$, where ε_g is the electron energy band gap, $\mathbf{k}$ is the wave vector, m_0 is the free electron mass, and $\underline{m}_e$ is the electron effective mass tensor. The band gap and components of the mass tensor are temperature dependent and they are taken from available experimental data[8, 9] . The hole band structure is

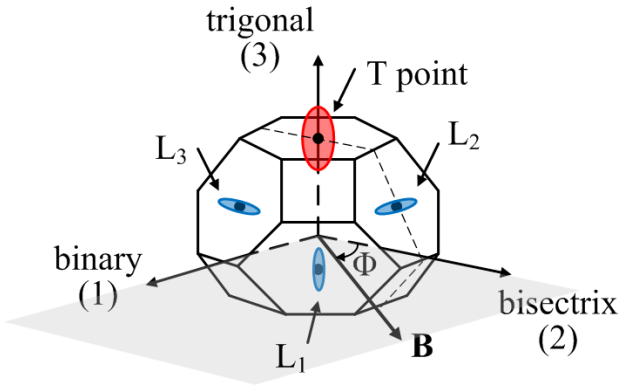

Fig. 1. Electron and Hole Fermi surfaces of bismuth at the Brillouin zone and the orientation of the externally applied magnetic field B.

described by a parabolic model: $\varepsilon_h(\mathbf{k}) = \frac{\hbar^2}{2m_0}\mathbf{k}\underline{m}_h^{-1}\mathbf{k}$, where $\underline{m}_h$ is the effective hole mass tensor with temperature independent components taken from available experiments[8]. We consider an external magnetic B field applied in the bb-plane, characterized by an angle Φ measured with respect to the bisectrix (Figure 1). The total conductivity tensor is

$$\underline{\sigma} = \sum_{i=1}^{3} \underline{\sigma}^{e,i} + \underline{\sigma}^{h} \tag{1}$$

where the electron and hole contributions are indexed by *e* and *h*, respectively, and *i* indicates summation over the L-pockets[10]. The partial conductivities are calculated by solving the Boltzmann equation within the relaxation time approximation:

$$\underline{\sigma}^{e,i(h)} = e^2 \int d\varepsilon \left(-\partial f_0/\partial\varepsilon\right) \underline{\Sigma}^{e,i(h)}(\varepsilon) \tag{2}$$

$$\underline{\Sigma}^{e,i(h)}(\varepsilon) = \frac{2}{(2\pi)^3}\int d^3k \underline{\mathbf{v}^{e(h)}(\mathbf{k})\mathbf{v}^{e(h)}(\mathbf{k})} \cdot \underline{\tau}^{e,i(h)}(\mathbf{k})\delta\left[\varepsilon - \varepsilon_{e,(h)}(\mathbf{k})\right] \tag{3}$$

where $\underline{\Sigma}$ is the partial distribution transport tensor, *e* is the electron charge, f_0 is the equilibrium Fermi-Dirac distribution function, $\mathbf{v}^{e(h)}(\mathbf{k}) = \hbar^{-1}\partial\varepsilon_{e(h)}(\mathbf{k})/\partial\mathbf{k}$ are the carriers' group velocity components, and $\underline{\tau}^{e,i(h)}(\mathbf{k})$ are the relaxation time tensors[7, 8, 11, 12]. The latter are expressed using the Mathiessen's rule as $\underline{\tau}^{e,i(h)} = \left(\left(\underline{\tau}_{intr}^{e(h)}\right)^{-1} + \left(\underline{\tau}_{B}^{e,i(h)}\right)^{-1}\right)^{-1}$, where the first term accounts for the

intrinsic scattering mechanisms and the second one represents the effects of the externally applied field B. $\underline{\tau}_{\text{int}\,r}^{e(h)}$ is diagonal with components assumed corresponding to dominant carrier-phonon scattering[13, 14]. Also[15], $\underline{\tau}_B^{e(h)} = e\underline{B}\underline{m}^{e(h),-1}$, where the nonzero components of the antisymmetric $\underline{B}$ tensor reflect the geometry in Figure 1: $B_{13} = -B_{31} = B\cos\Phi$ and $B_{32} = -B_{-23} = B\sin\Phi$. Evaluating Eq. (3) leads to:

$$\Sigma_{33}^{e,i(h)} = \frac{A^{e(h)}B^{e(h)}}{C^{e(h)} + D^{e(h)}\cos^2\left(\Phi + (i-1)\frac{2\pi}{3}\right)} \tag{4}$$

where

$$A^{e(h)} = \frac{2\tau_3^{e(h)}}{3\pi^2\hbar^3}\left(\frac{2m_1^{e(h)}m_2^{e(h)}}{m_3^{e(h)}}\right)^{1/2} \tag{5}$$

$$B^e = \frac{\gamma^{3/2}d\gamma/d\varepsilon_e}{2(1+4\gamma/\varepsilon_g)}, \qquad B^h = \varepsilon_h^{3/2} \tag{6}$$

$$C^{e(h)} = 1 + \frac{e^2B^2\tau_2^{e(h)}\tau_3^{e(h)}}{m_2^{e(h)}m_3^{e(h)}} \tag{7}$$

$$D^{e(h)} = \frac{e^2B^2\tau_3^{e(h)}}{m_1^{e(h)}m_2^{e(h)}m_3^{e(h)}}(m_2^{e(h)}\tau_1^{e(h)} - m_1^{e(h)}\tau_2^{e(h)}) \tag{8}$$

and $\gamma = \varepsilon_e(1+\varepsilon_e/\varepsilon_g)$. The electron and hole mass components along the bisectrix, binary, and trigonal axes are denoted as $m_{1,2,3}^{e,h}$, respectively. Together with ε_g, these are taken from available experimental data[8, 9]. The relaxation times $\tau_{1,2,3}^{e(h)}$ and the Fermi levels for the carriers $\varepsilon_F^{e(h)}$ are determined such that the zero-field calculated properties fit those experimentally measured in Ref. [16] for bulk bismuth in the temperature range 80 K to 300 K. The obtained values are shown in Table I.

Table 1. Obtained values for the electron and hole Fermi levels and scattering times for different temperatures along the binary, bisectrix, and trigonal directions. The obtained relaxation phonon scattering times along the trigonal direction are also given.

T(K)	ε_F^e(eV)	ε_F^h(eV)	$\tau_{0,1}^e$ (10^{-13}s)	$\tau_{0,2}^e$ (10^{-13}s)	$\tau_{0,3}^e$ (10^{-13}s)	$\tau_{0,1}^h=\tau_{0,2}^h$ (10^{-13}s)	$\tau_{0,3}^h$ (10^{-13}s)	$\tau_{0,3}^{ph}$ (10^{-9}s)
80	0.029	0.0154	18.995	51.421	92.239	71.709	221.026	21.244
100	0.031	0.0157	12.054	32.629	57.069	49.642	149.186	20.739
120	0.033	0.0158	8.163	22.099	37.908	37.287	109.902	18.352
140	0.036	0.0159	5.506	14.906	24.830	28.905	82.731	16.196
160	0.039	0.0160	3.837	10.388	17.453	22.343	64.499	12.394
180	0.043	0.0170	2.731	7.392	12.236	17.413	49.523	9.131
200	0.049	0.0195	1.958	5.301	8.617	13.284	37.106	6.592
220	0.054	0.0236	1.414	3.829	6.179	9.833	27.162	4.031
240	0.060	0.0286	1.031	2.791	4.518	7.376	20.522	2.015
260	0.066	0.0360	0.747	2.022	3.241	5.410	14.895	0.959
280	0.074	0.0449	0.540	1.462	2.347	3.984	10.989	0.485
300	0.081	0.0572	0.382	1.034	1.627	2.886	7.801	0.280

III. Calculated Transport Properties

In Figure 2a the angular dependence of the resistivity $\rho_{33} = \sigma_{33}^{-1}$ along the trigonal axis is shown. The oscillations for the displayed temperature range are related directly to the $\cos^2(\Phi + (i-1)2\pi/3)$ dependence in Σ_{33}. As the field rotates in the bb-plane, the different L-pockets will contribute with different strengths, so that ρ_{33} exhibits periodic minima and maxima. The factor D^e in Eq. (8) is a measure of the electron mass anisotropy determining the

magnitude of the oscillations. This anisotropy can further be enhanced if B is increased. However, for holes $m_1^h = m_2^h$ and $\tau_1^h = \tau_2^h$ (Table I), thus the orientation of the field does not affect their transport[8]. The results in Figure 2a are in agreement with the reported measurements for bismuth[6]. The field angular dependence and even the oscillations magnitude are well reproduced. This is strong experimental validation of this model.

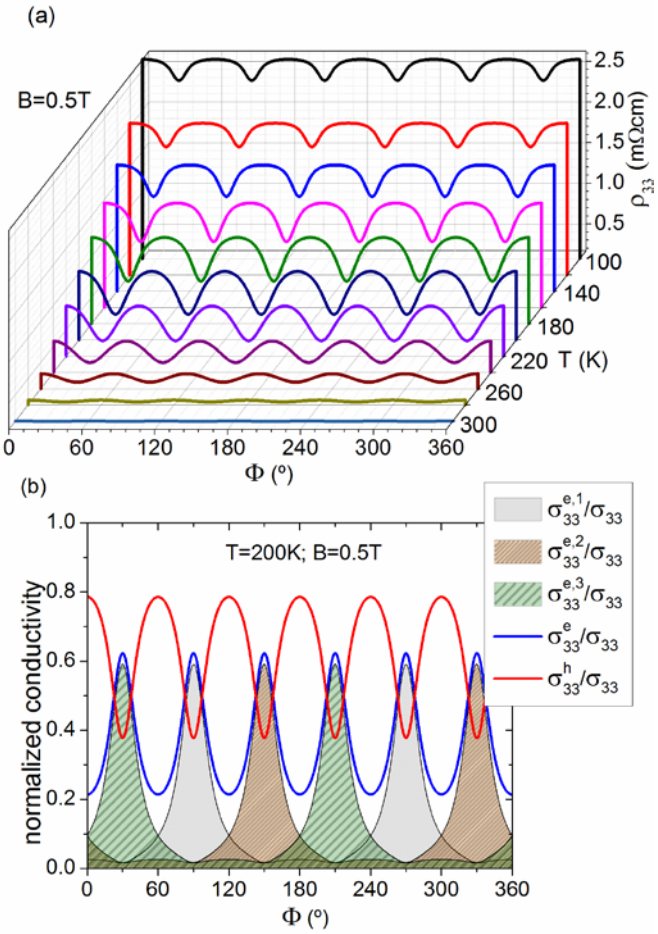

Fig. 2 (a) The electrical resistivity along the trigonal direction as a function of the B field orientation for different temperatures; (b) Conductivity of electronic and hole pockets normalized to the total charge conductivity along the trigonal direction. The normalized total electronic conductivity is also shown.

Figure 2b shows that each L-pocket will be responsible for approximately 60% of σ_{33} at $\Phi = (2n+1)\pi/6$, while the holes account for the rest ($n \in [0,6]$ is integer). σ_{33}^e of each L-ellipsoid acquires its largest value when the field is oriented along the binary axis, which is perpendicular to the longer axis of that ellipsoid. As B rotates, σ_{33}^e decreases until the field becomes parallel to the longer axis of the ellipsoid. The hole contribution to σ_{33}^e is approximately 80% at those Φ for which the L-pockets contribution is minimum. The field magnitude and temperature also contribute significantly to the relative balance of $\sigma_{33}^{e,i}$ and σ_{33}^h to σ_{33}. Larger B and lower T will increase the magnitude of the maxima of the L-pockets, while smaller B and higher T reduce the oscillations, as seen in Figure 2.

These findings indicate that the transport can be effectively polarized by applying a magnetic field in the bb-plane. The field breaks the symmetry of the three L-ellipsoids, and as its direction changes, electrons residing in particular valley can be stimulated, while the others are suppressed. The main reason for this behavior is the electron mass anisotropy along the binary and bisectrix axes. We further demonstrate that it is not only possible to obtain specific Dirac valley polarization of the conductivity, but other transport characteristics exhibit similar features. The Seebeck coefficient is calculated next using

$$\underline{S} = \left(\sum_{i=1}^{3} \underline{\sigma}^{e,i} \underline{S}^{e,i} + \underline{\sigma}^{h} \underline{S}^{h} \right) \underline{\sigma}^{-1} \tag{9}$$

$$T\left(\underline{\sigma}^{e,i(h)} \cdot \underline{S}^{e,i(h)} \right) = e \int d\varepsilon \left(-\partial f_0 / \partial \varepsilon \right) \underline{\Sigma}^{e,i(h)}(\varepsilon)(\varepsilon - \mu) \tag{10}$$

where $\underline{S}^{e,i(h)}$ are the partial electron and hole Seebeck coefficients, and μ denotes the chemical potential. The angular dependence of $S_{33}^{e(h)}$ and the total S_{33} are shown in Figure 3a. Since the in-plane hole masses are isotropic, S_{33}^{h} is not affected by the orientation of the in-plane field. The inset of Figure 3a shows that the magnitude of the S_{33}^{e} oscillations is small, but because of the large oscillations in the conductivities (Eq. 9), S_{33} exhibits similar field angular behavior as in Figure 2a. $|S_{33}|$ is maximum when ρ_{33} is maximum, and these correspond to the dominant contribution of carriers residing in the specific electronic valleys as shown in Figure 2b. The Seebeck coefficient is positive when the hole contribution to σ_{33} is larger and it changes its sign when the electrons dominate.

The limits of the angular oscillations of S_{33} as a function of the field strength for various temperatures reveal a different aspect of the transport (see Figure 3b). For lower T (T=100K) and sufficiently high B, the holes always dominate the transport, since S_{33} is always positive. For higher T (T=300K), the electrons dominate the transport and S_{33} is negative for all Φ. There is an intermediate regime (T=200K and 0.25T<B<0.75T) when the two carrier contributions will be comparable and S_{33} will periodically change sign as the field rotates. These findings illustrate how to further control the transport in bismuth: for intermediate temperatures, the orientation and magnitude of the field in the bb-plane can be used not only for valley polarization, but also for selective filtering of the carriers type.

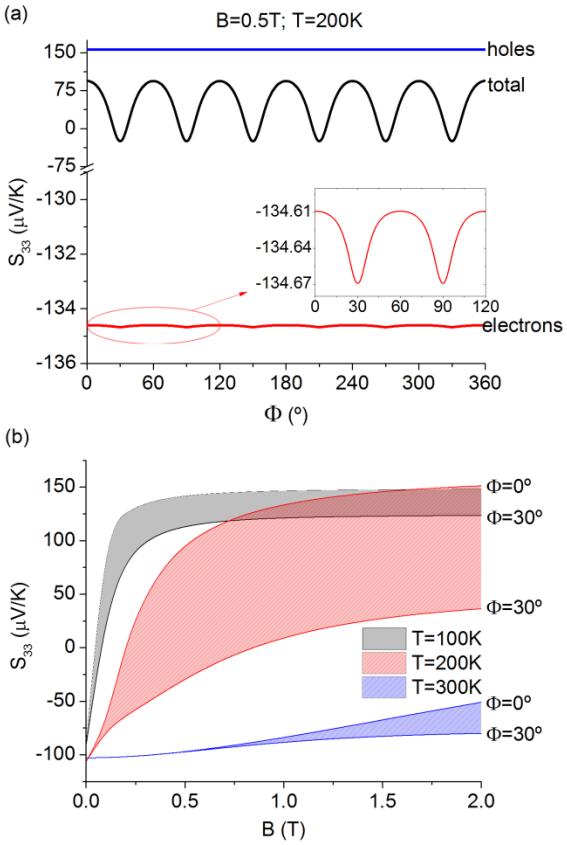

Fig. 3 (a) The angular dependence of the total and partial Seebeck coefficients; (b) Seebeck coefficient oscillations amplitude as a function of the magnetic field strength for different temperatures.

We also evaluate the thermal conductivity as

$$\underline{\kappa} = \sum_{i=1}^{3} \underline{\kappa}^{e,i} + \underline{\kappa}^{h} + T\underline{\sigma}^{e}\underline{\sigma}^{h}\left(\underline{S}^{h} - \underline{S}^{e}\right)^{2}\underline{\sigma}^{-1} + \underline{\kappa}^{L} \tag{11}$$

$$\underline{\kappa}^{e,i(h)} = \int d\varepsilon \left(-\partial f_0/\partial\varepsilon\right)\underline{\Sigma}^{e,i(h)}(\varepsilon)(\varepsilon-\mu)^2/T - T\underline{S}^{e,i(h);T}\cdot\underline{\sigma}^{e,i(h)}\cdot\underline{S}^{e,i(h)} \tag{12}$$

where $\underline{\kappa}^{e,i}$ and $\underline{\kappa}^{h}$ correspond to the electronic and hole contributions given in Eq. (12). The third term accounts for the bipolar diffusion characteristic for materials with two types of carriers carrying heat in the same direction. $\underline{\kappa}^{L}$ represents the lattice thermal conductivity and is calculated within the Holland-Callaway model and the relaxation time approximation[17, 18]. The zero-field $\underline{\kappa}$ found via Eqs. (11,12) reproduces the experimental data reported in Ref. [15], and in Table 1 we give the phonon relaxation scattering times along the trigonal axis.

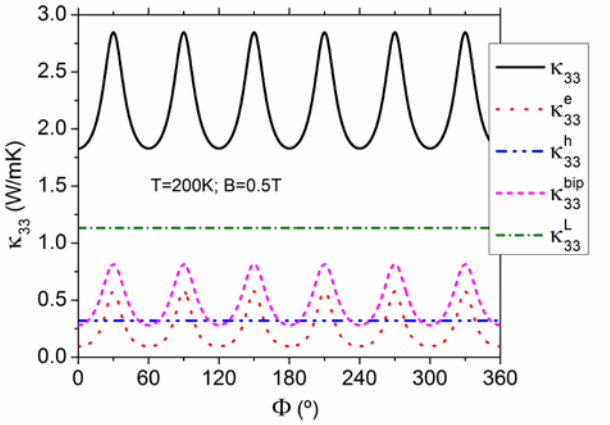

Fig. 4. The angular dependence of the thermal conductivity along the trigonal direction.

Figure 4 shows that κ_{33} also exhibits oscillations with the applied magnetic field orientation with maxima corresponding to the minima of S_{33} and ρ_{33}. κ_{33}^{L} is independent of the field and its value is the experimental one for the trigonal direction at T=200 K in Ref. [16]. κ_{33}^{h} is also independent of the field orientation. κ_{33}^{e} has angular oscillations and its contribution to the total total thermal conductivity will vary, depending on the field orientation. For magnetic fields oriented along the binary axis κ_{33}^{e} is larger, whereas for fields oriented along the bisectrix, κ_{33}^{h} is larger. Since the bipolar term accounts for the heat transported by pairs of electrons and holes, its contribution to κ_{33} has maxima at fields orientations where κ_{33}^{e} has the largest values.

Finally, we consider the thermoelectric performance of bismuth, described via the dimensionless figure of merit $ZT_{33} = S_{33}^2 \sigma_{33} T / \kappa_{33}$, as a function of the magnetic field orientation. This dimensionless quantity is directly related to the efficiency of thermoelectric devices as large ZT values imply better performance. The polar representation in Figure 5a shows that the repeating maxima of ZT_{33} for B=0.5T occur at those Φ for which σ_{33} and κ_{33} are maximum (S_{33} is minimum), however for B=0.2T ZT_{33} is maximum for those Φ for which S_{33} is maximum (σ_{33} and κ_{33} are minimum). Figure 5b presents a different perspective of the ZT_{33} dependence on the field orientation. For T=200K, for a small B field, the figure of merit is maximized for $\Phi = 30^0$ and minimized for $\Phi = 0^0$. For a larger field (B>0.3T), the situation is reversed. This is a consequence of the relative contribution of σ_{33} and κ_{33} (as opposed to S_{33}) in their ratio comprising ZT_{33}.

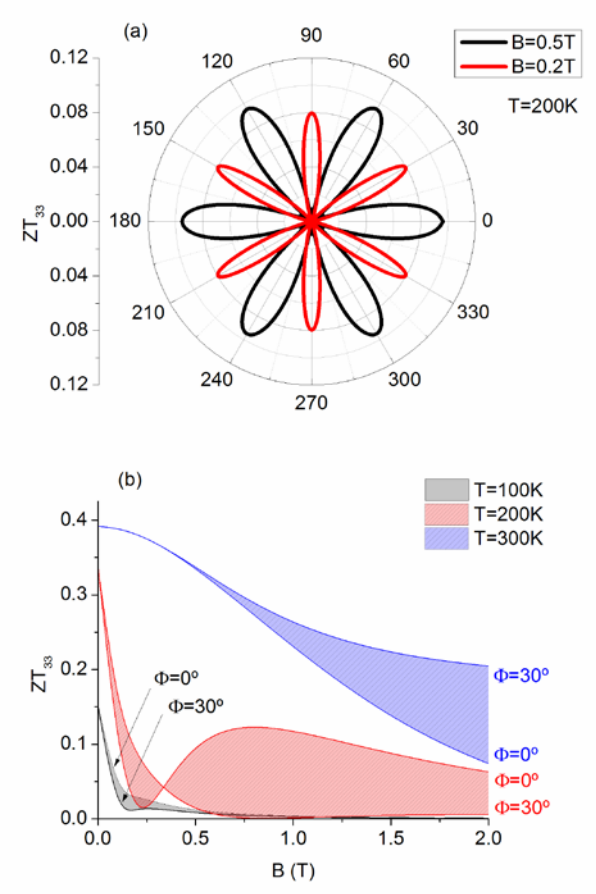

Fig. 5. The thermoelectric figure of merit along the trigonal direction: (a) polar representation of its angular dependence, and (b) limits of its oscillations amplitude for different temperatures.

IV. Summary

In summary, we have demonstrated that a magnetic field in the bb-plane can excite single Dirac valleys with signatures in different transport characteristics. Consequently, the bismuth

thermoelectricity can be further controlled by tuning the type of carriers dominating the transport and its overall figure of merit.

Acknowledgements

A. Popescu acknowledges support under the Cooperative Research Agreement between the University of Maryland and the National Institute of Standards and Technology Center for Nanoscale Science and Technology, Award 70NANB10H193, through the University of Maryland. L. M. Woods acknowledges financial support from the National Science Foundation under contract CBET-0932526. Communications with K. Behnia are also acknowledged.

References:

[1] A. Rycerz, J. Tworzydlo, C.W.J. Beenakker, *Nature Phys.* **2007**, 3, 172

[2] T. Low, F. Guinea, *Nano Lett* **2010**, 10, 3551.

[3] J.L. Garcia-Pomar, A. Cortijo, M. Nieto-Vesperinas, *Phys. Rev. Lett.* **2008**, 100, 236801.

[4] N.C. Bishop, M. Padmanabhan, K. Vakili, Y.P. Shkolnikov, E.P. De Poortere, M. Shayegan, *Phys. Rev. Lett.* **2007**, 98, 266404.

[5] K. Takashina, Y. Ono, A. Fujiwara, Y. Takahashi, Y. Hirayama, *Phys. Rev. Lett.* **2006**, 96, 236801.

[6] Z. Zhu, A. Collaudin, B. Fauque, W. Kang, K. Behnia, *Nature Phys.* **2012**, 8, 89.

[7] M.H. Cohen, *Phys. Rev.* **1961**, 121, 387.

[8] M.P. Vecchi, M.S. Dresselhaus, *Phys. Rev. B* **1974**, 10, 771.

[9] Y. Liu, R.E. Allen, *Phys. Rev. B* **1995**, 52, 1566.

[10] J.M. Ziman, *Electrons and Phonons* (Oxford Univ. Press, 1960).

[11] W.S. Boyle, G.E. Smith, *Prog. Semicond*. **1963**, 7, 1.

[12] V.S. Edelman, *Adv. Phys.* **1976**, 25, 555.

[13] J. Heremans, O.P. Hansen, *J. Phys. C* **1979**, 12, 3483.

[14] A. Popescu, L.M. Woods, *Phys. Rev. B*, to be published.

[15] I. F. I. Mikhail, O. P. Hansen, H. Nielsen, J. Phys. C **1980**, 13, 1697.

[16] C.F. Gallo, B.S. Chandrasekhar, P.H. Suter, *J. Appl. Phys.* **1963**, 34, 144.

[17] J. Callaway, *Phys. Rev.*, **1959**, 113, 1046.

[18] M.G. Holland, *Phys. Rev.* **1963**, 132, 2461.